IEEE Access
Multidisciplinary | Rapid Review | Open Access Journal

Received September 13, 2018, accepted October 16, 2018, date of publication October 22, 2018,
date of current version November 19, 2018.

Digital Object Identifier 10.1109/ACCESS.2018.2877297

Compact High Q Configurable Quint-Band Electromagnetic Bandgap Filter

YU GUO[1,2], (Member, IEEE), SUNGJUN KIM[2], HUAI GAO[1], (Senior Member, IEEE), AND GUANN-PYNG LI[2], (Member, IEEE)

[1]School of Physics, Nanjing University, Nanjing 210093, China
[2]Department of Electrical Engineering and Computer Science, University of California at Irvine, Irvine, CA 92697, USA

Corresponding author: Yu Guo (icr_gy@hotmail.com)

This work was supported in part by the Natural Science Foundation of Jiangsu Province under Grant BK20160190, in part by the Fundamental Research Funds for the Central Universities under Grant JUSRP11740, in part by the Natural Science Foundation of China under Grant 61701195, and in part by the Chinese Postdoctoral Science Foundation under Grant 2017M621710.

ABSTRACT A compact quint-band bandpass filter using an electromagnetic bandgap (EBG) material is proposed. To the best of authors' knowledge, this is the first quint-band filter using the EBG material. The quint-band EBG filter consists of EBG substrate and five sets of lumped capacitors. In comparison with other quint-band filters using stepped impedance resonator, the EBG filter has advantages including high Q, a wide stopband, and good band-to-band isolation. The employment of external capacitors makes it possible to control each passband's working frequency. This paper provides a simple and effective method to design a quint-band filter with a low insertion loss and a compact size. Experimental verification is provided, and a good agreement has been found between simulation and measurement. The measured return loss of the five passbands is better than 13.0 dB, and band-to-band isolation is better than 29.0 dB. The spurious signal suppression in the upper frequency range from 3.36 to 10.0 GHz is higher than 20.0 dB.

INDEX TERMS EBG filter, quint-band, high Q, compact size, frequency controllable.

I. INTRODUCTION

In the process of rapid evolution into microwave wireless communication, the demand for multi-band/multi-functional microwave systems that support various modern services has increased rapidly. Such systems require microwave circuits and components can handle several different frequency bands.

Multi-band filters have been researched intensively and various design approaches have been proposed [1]–[8]. A miniaturized quad-band bandpass filter (BPF) was implemented on high-k substrate by using screen-printing technique [1]. In [3], two types of dual-band BPFs were designed and combined to realize a quad-band BPF. In [4], by using asymmetric stepped-impedance resonator (SIR), stopband bandwidth of the quad-band BPF is extended. To improve frequency selectivity, meandering structures are utilized to suppress un-wanted passbands or obtain transmission zeroes in [5]. However, there has been little research about quint-band and sext-band BPFs in the past literature [6]–[8]. This is because, for the quint-band and sext-band case, it is usually difficult to simultaneously satisfy all the design conditions required for the five and six bands. A double-layered structure with more design flexibility is utilized to provide a multipath for different bands in [6]. In [8], a tri-mode stub-loaded SIR was utilized to implement a third-order BPF with a transmission zero near the passband.

To the best of authors' knowledge, most of the reported quad-band, quint-band, sext-band BPFs are using SIR. Due to moderate selectivity of SIR and its spurious passbands, resonators are designed with different structures to suppress the spurious passband [4], [5] or introduce transmission zeros [5]–[8] for improving selectivity. Therefore, the reported filters presented good electrical performances while noticing that circuit sizes and structures complex were compromised.

In this paper, a high Q configurable quint-band electromagnetic bandgap (EBG) filter is proposed extending our previous work [9]. A quint-band filter is constructed by EBG material and lumped capacitors using two-layer PCB manufacturing technique. The employment of external capacitors makes it possible to control each passband's working frequency. Specific working frequency can be chosen on demand by changing capacitor's value. Compared with previous work, the proposed filter has advantages of compact size, a wide stopband, good band to band isolation, and easy fabrication.

II. CEBG RESONATOR DESIGN

Implemented in a common two-layer PCB, the 3D diagram of configurable electromagnetic bandgap (CEBG) resonator is shown in Fig. 1(a). Energy transition and coupling circuits are designed on the top copper layer of PCB as depicted in Fig. 1(b). This circuit utilizes Co-Planar Waveguide (CPW) on top plate to couple energy into the EBG substrate [10].

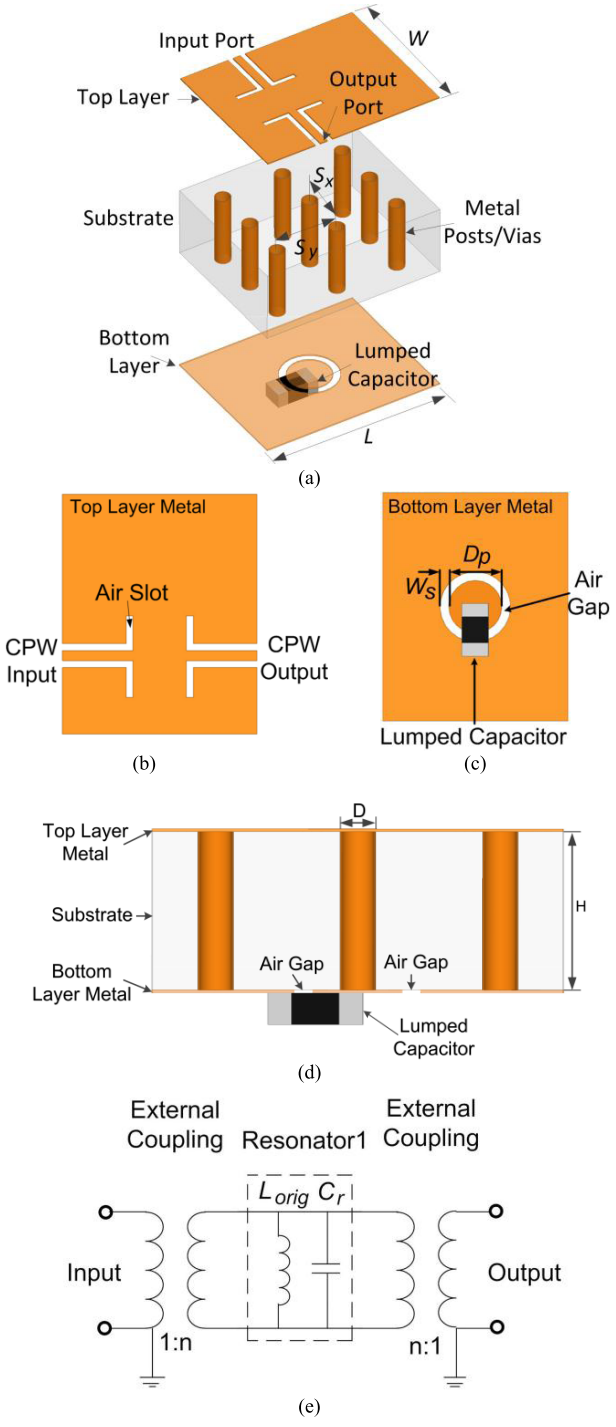

FIGURE 1. Schematic of proposed resonator design: (a) PCB with generalized lumped capacitor as loading element; (b) Top view of the proposed resonator; (c) Bottom view of the resonator; (d) Cross section view of the resonator; (e) Equivalent circuit model of the resonator.

Electroplated copper posts serve as the periodic lattice in EBG substrate and connect the top layer with the bottom one. Spacing between posts was firstly determined by following what has been published in [11]. In order to achieve a compact size, the spacing then is significantly reduced based on scalable properties of EBG structure. This is because, in a scaled EBG material, new electromagnetic mode and its frequency can be obtained by simply rescaling the old electromagnetic mode and its frequency [12]. EM simulation was used to determine final spacing between those posts. High pass resonator is created by evanescent sections which confine fields inside. The small spacing between posts also contributes to an effective energy confinement. A broad electromagnetic bandgap is contributed by those periodic posts, so that a wide spurious free range can be obtained by the resonator. $Q_{radiation}$ of corresponding resonator is extracted from simulation results by commercial EM software Ansoft HFSS. As presented in [9], $Q_{radiation}$ approximately equals to Q_u (unloaded quality factor) which is 41000 at 3.50 GHz.

One air gap separating metal pad from surrounding ground plane in the bottom copper layer is used for surface mounted capacitor as depicted in Fig. 1(c). Lumped capacitor surface mounted between the metal pad and RF (radio frequency) signal ground is connecting in parallel with copper post standing on the metal pad and *LC* resonance is contributed by the parallel circuits. The resonator's resonant frequency is mainly determined by capacitance of a surface mounted capacitor and inductance attributed to copper post connected with the lumped capacitor. The final cross section of the CEBG resonator is shown in Fig. 1(d).

An equivalent circuit model of the resonator is developed and shown in Fig. 1(e). It consists of one parallel *LC* resonator with input and output transformers which represent external energy coupling. The C_r of this resonator is given by:

$$C_r = C_{orig} + C_{lumped} \tag{1}$$

The resonant frequency can be approximated by:

$$\omega = \frac{1}{\sqrt{L_{orig}(C_{orig} + C_{lumped})}} \tag{2}$$

In (2), C_{lumped} is capacitance value of surface mounted lumped capacitor, L_{orig} and C_{orig} stand for original inductance and capacitance of EBG substrate, respectively. Q_u of the resonator is given by:

$$Q_u = \left(\frac{1}{Q_{conductor}} + \frac{1}{Q_{dielectric}} + \frac{1}{Q_{radiation}}\right)^{-1} \tag{3}$$

In (3), $1/\ Q_{dielectric} = \tan\delta$ which is loss tangent of filter's substrate material. From (2), it is noted filter's working frequency depends on lumped capacitor's value, which can be changed to tune the filter's frequency. Since the filter's tuning frequency range depends on the external capacitors and since it does not rely on size and height of via post, the resonator's

size can be significantly reduced. This design allows for an increased degree of design freedom.

By utilizing commercial EM software Ansoft HFSS, a resonator with dimensions shown in Table 1 is simulated and the simulation results are shown in Fig. 2. Please note the length and width of the resonator are only 2.5 mm and 2.0 mm respectively. Q_u can be extracted from the simulation results using equations (4-6) [13].

$$Q_{loaded} = \frac{f_0}{\Delta f} \tag{4}$$

$$Q_{external} = 10^{-[S_{21}(dB)/20]} \cdot Q_{loaded} \tag{5}$$

$$Q_u^{-1} = Q_{loaded}^{-1} - Q_{external}^{-1} \tag{6}$$

TABLE 1. CEBG resonator dimensions.

Parameters	L	W	S_x	S_y	D_P	W_S	D
Value/mm	*2.5*	2.0	*0.65*	*0.9*	*0.38*	*0.11*	*0.2*

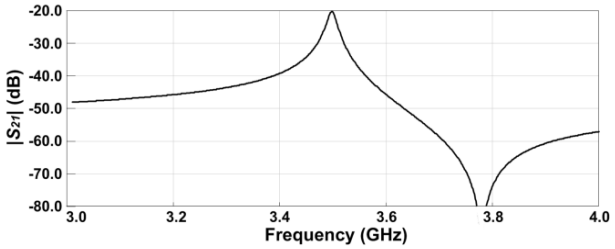

FIGURE 2. Simulated $|S_{21}|$ of the CEBG resonator with high Q surface mount capacitor.

The extracted Q_u of the resonator is 234 ($\Delta f = 16.6$ MHz and $S_{21} = -20.04$ dB).

A wide spurious free range of the resonator is obtained shown in Fig. 3. The resonator's upper stopband with -35 dB attenuation level is extended to 40.0 GHz. Simulated electric and magnetic fields of the resonator are shown in Fig. 4. As can be seen in Fig. 4(a), magnetic fields mainly surround a middle post standing on bottom metal pad. At resonance frequency, signal current flows through the middle post and surface mounted lumped capacitor. To simulate electric fields of the resonator, lumped RLC boundary is used to represent surface mounted lumped capacitor. The RLC boundary was applied between the circular metal pad and RF signal ground.

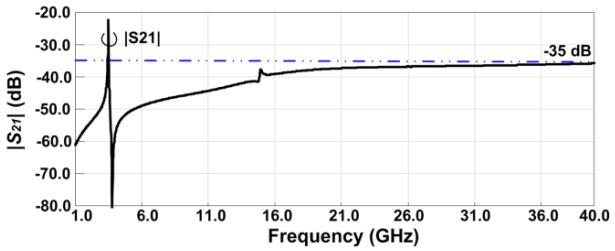

FIGURE 3. Simulated $|S_{21}|$ and wide stopband of the CEBG resonator.

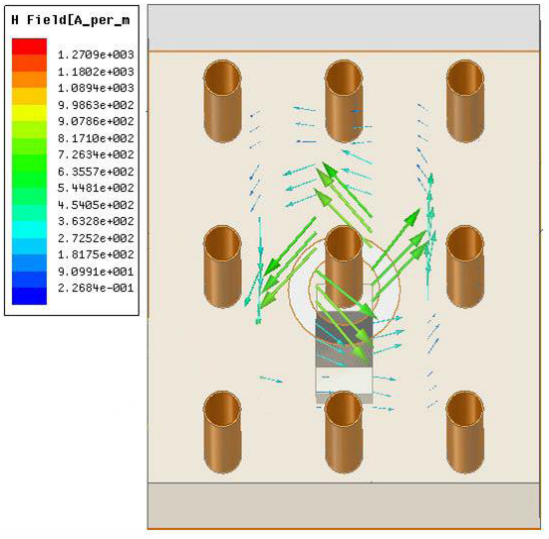

(a)

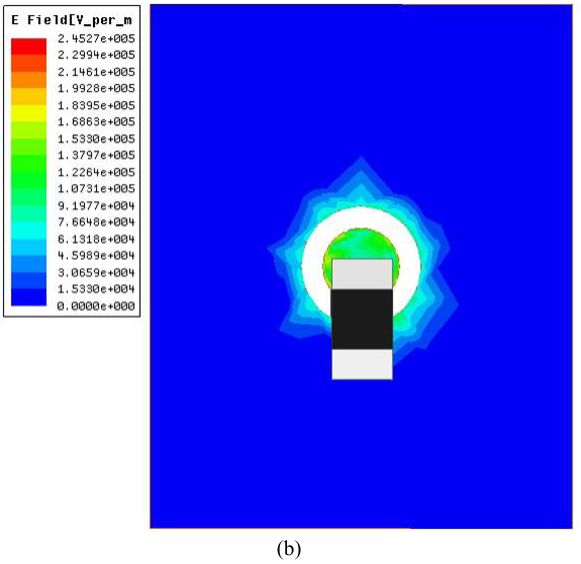

(b)

FIGURE 4. Magnetic and electric fields in a single resonator: (a) Magnetic field vectors; (b) Electric fields.

The simulation result is shown in Fig. 4(b). Electric field mainly concentrated around the surface mounted lumped capacitor.

III. CEBG QUINT-BAND FILTER DESIGN

By integrating five pairs of CEBG resonators, 3D diagram of the designed quint-band filter is shown in Fig. 5. As shown in Fig. 5(a), energy transition and coupling circuit is designed on top layer. Please note that to obtain low insertion loss of all five passbands, energy coupling circuit not only requires to couple energy for all the resonators but also requires to have a broadband coupling capability since the passbands are located in a wide frequency range. In order to avoid energy concentrating on few of the resonators which lead to a big difference regarding insertion loss for five passbands, a CPW power divider following the design procedure outlined in [14]

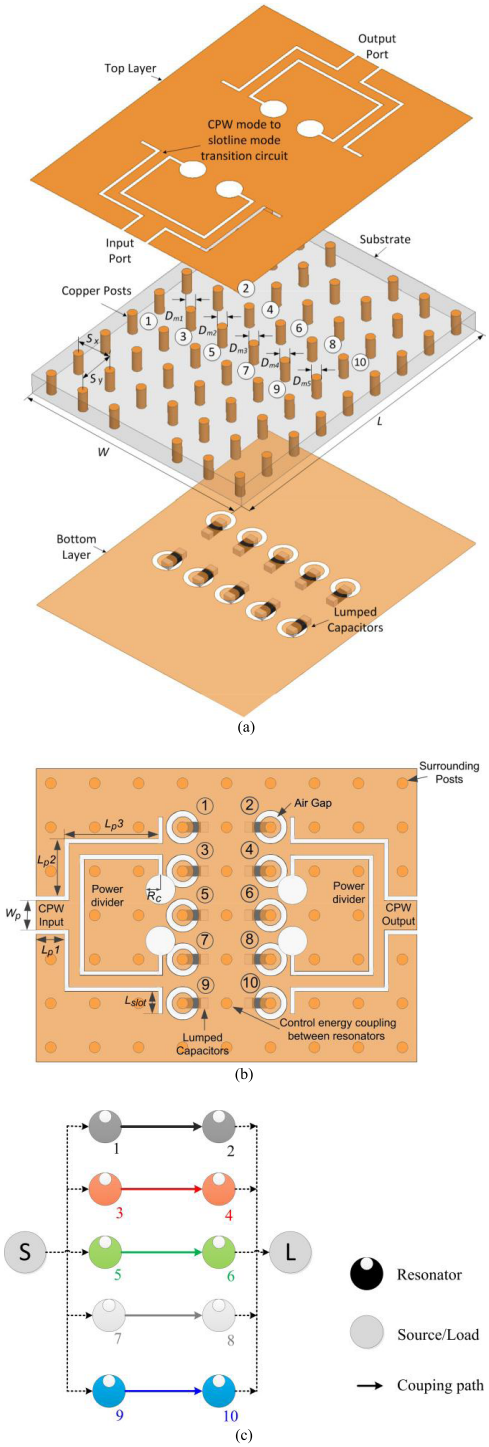

FIGURE 5. Schematic of a quint-band CEBG filter design: (a) 3D diagram of a quint-band filter with generalized lumped capacitors surface mounted on bottom plate of the filter; (b) Top view of the proposed filter; (c) Coupling structure of the proposed quint-band BPF.

is used to equally separate and couple energy to all resonators as shown in Fig. 5(a). Energy transmitted through the CPW power divider is required to be transformed from CPW mode to slotline mode for efficient energy coupling. To enhance coupling efficiency to the EBG substrate, an electric short circuit at the end of the CPW and a co-existing electric open circuit of slotline are required. While different CPW to slotline transition circuits had been analyzed and demonstrated with a relative broadband [15], their sizes are not suitable for integration and energy coupling in compact filters design. A CPW to slotline transition and coupling circuit is redesigned shown in Fig. 5 for achieving both broadband performance and compact size. Broadband energy transition and coupling is achieved by utilizing circular open slots [16].

This proposed filter has five sets of resonators as shown in Fig. 5(b). The resonant posts are standing on metal pad and connecting with lumped capacitors. The first one consists of Res1 (Resonator1) and Res2 working at the same frequency and determines the first working frequency band of the filter. Resonator (3, 4)/(5, 6)/(7, 8)/(9, 10), represent the second, third, fourth, and fifth set respectively and contribute to other four frequency bands. Please note that these ten resonators share a common EBG substrate with a compact size. The surrounding copper vias are preventing energy from leaking out. Fig. 5(c) shows the coupling structure of the proposed circuits, wherein the gray circle indicates the source and load, the black circle means a CEBG resonator, the dot line represents the coupling between feeding lines and resonators, and the solid line indicates the magnetic coupling between resonators. The posts between two resonators can be used to control magnetic energy coupling between those resonators. The value denotes the channel number. It is clear that each passband can be designed independently by a set of resonators.

In this study, resonator (1, 2)/(3, 4)/(5, 6)/(7, 8)/(9, 10) operate at 1.53, 1.9, 2.35, 2.86, and 3.3 GHz, respectively. The fractional bandwidths of these five channels are $FBW_1 = 1.91\ \%$, $FBW_2 = 1.13\ \%$, $FBW_3 = 1.62\ \%$, $FBW_4 = 1.05\ \%$, and $FBW_5 = 0.97\ \%$. For 0.1 dB Chebyshev response, the element values are $g_0 = 1$, $g_1 = 0.8431$, $g_2 = 0.622$, $g_3 = 1.3554$.

Based on the above specification, the design parameters are determined. 11.6, 7.9, 4.8, 3.5, and 2.5 pF capacitors are surface mounted for the first to fifth set of resonators respectively. The required coupling coefficients can be obtained by $M_{ij} = FBW_n/(g_1 g_2)^{0.5}$, n = 1, 2, 3, 4, 5 [17], where M_{ij} is the coupling coefficients between resonator i and resonator j. The required coupling coefficients are $M_{1,2} = 0.018$, $M_{3,4} = 0.012$, $M_{5,6} = 0.017$, $M_{7,8} = 0.011$, and $M_{9,10} = 0.0104$. Fig. 6 shows the extracted coupling coefficient versus the diameters D_{mi} including D_{m1}, D_{m2}, D_{m3}, D_{m4}, and D_{m5}. The diameters of posts between resonators can be designed based on the required coupling coefficients. The input/output external quality factor can be found as $Q_{en,in} = g_0 g_1/FBW_n = g_2 g_3/FBW_n = Q_{en,out}$, where Q_{en} represents the external quality factor for each passband, and they are $Q_{e1,in} = 44.14 = Q_{e1,out}$, $Q_{e2,in} = 74.61 = Q_{e2,out}$, $Q_{e3,in} = 52.04 = Q_{e3,out}$, $Q_{e4,in} = 80.29 = Q_{e4,out}$, and $Q_{e5,in} = 86.92 = Q_{e5,out}$. The length of coupling slotline and radius of coupling circular slot determine the required external quality factor.

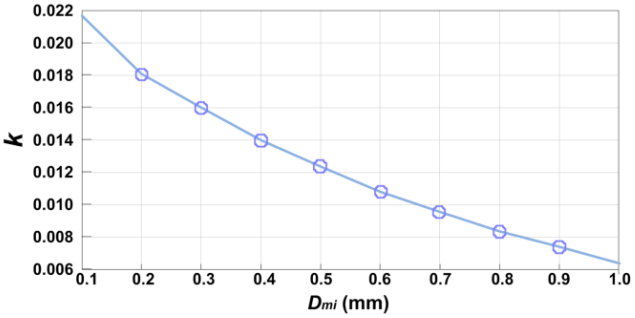

FIGURE 6. Extracted coupling coefficients.

By utilizing commercial EM software Ansoft HFSS, a quint-band filter is simulated with optimized dimensions shown in Table 2.

TABLE 2. CEBG quint-band filter dimensions.

Parameters	Value/mm	Parameters	Value/mm
L	52.0	W_S	0.3
W	40.0	D_P	1.8
S_x	6.0	L_{slot}	3.0
S_y	6.0	W_p	1.62
D_{m1}	0.95	L_p1	4.0
D_{m2}	1.06	L_p2	7.8
D_{m3}	1.0	L_p3	13.0
D_{m4}	1.18	D	1.2
D_{m5}	1.3	R_c	2.0

The filter's S parameters are simulated shown in Fig. 7. Keeping the other four passband's capacitor of 7.9 pF, 4.8 pF, 3.5 pF, 2.5 pF unchanged and increasing the first passband's capacitor's value from 10.6 to 12.2 pF, its center frequency is shifted from 1.57 to 1.49 GHz and the insertion loss is increased from 1.2 to 1.5 dB, while performances of other four passbands are barely changed. Please note magnetic energy coupling dominates between resonators and the passband's fractional bandwidth is determined by magnetic energy coupling coefficient between resonators. Consequently, even though lumped capacitor changes, the passband's fractional bandwidth is not changed as shown in Fig. 7(a). Similarly, when changing the second passband's capacitance value from 8.7 to 7.1pF and keeping the other four passbands' capacitors unchanged, the second passband's center frequency shifts from 1.78 to 1.91 GHz and insertion loss increases from 0.87 to 0.95 dB. Again it is noted that performances of other four passbands are barely changed. Control of the third, fourth, and fifth passband's center frequency is shown by Fig. 7(c), Fig. 7(d), and Fig. 7(e) respectively. It is clear from those simulation results that keeping four passband's capacitance unchanged and changing the rest one's capacitor value, its center frequency shifts with little influence on performance of other four passbands.

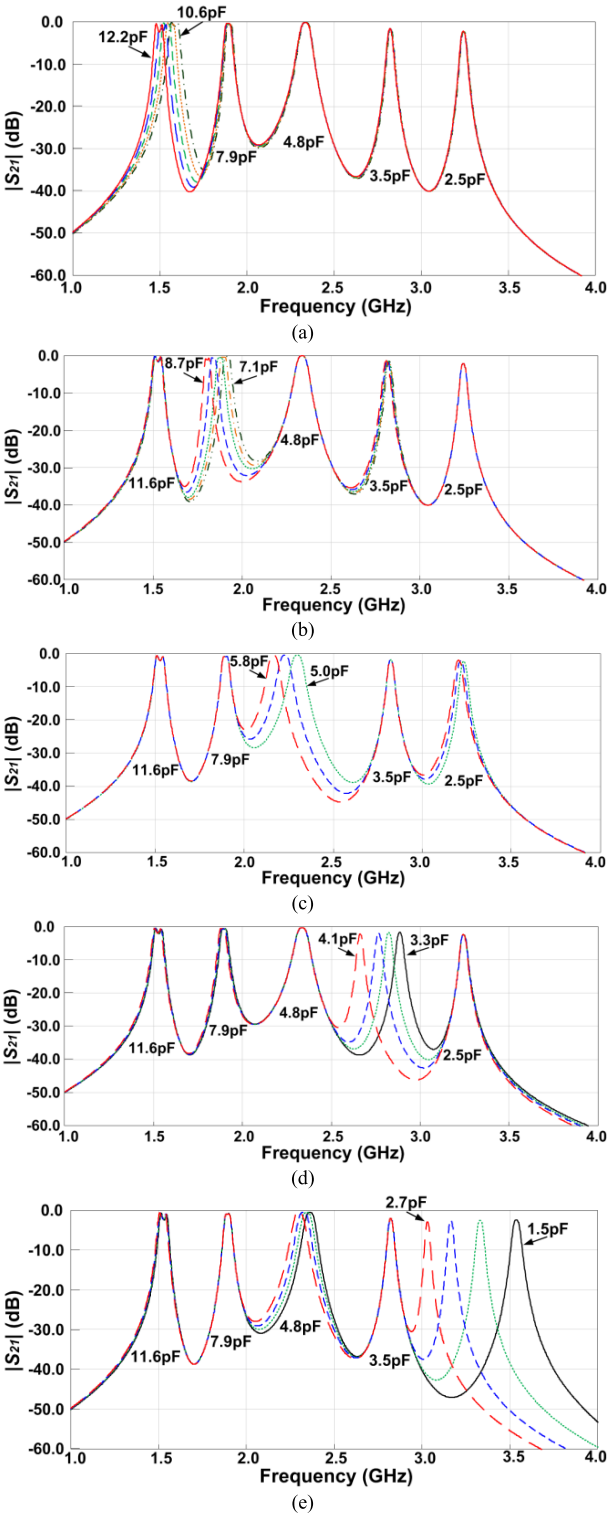

FIGURE 7. Simulated working frequency change of each passband with little influence on other passbands: (a) First passband; (b) Second pandband; (c) Third passband; (d) Forth pandband; (e) Fifth passband.

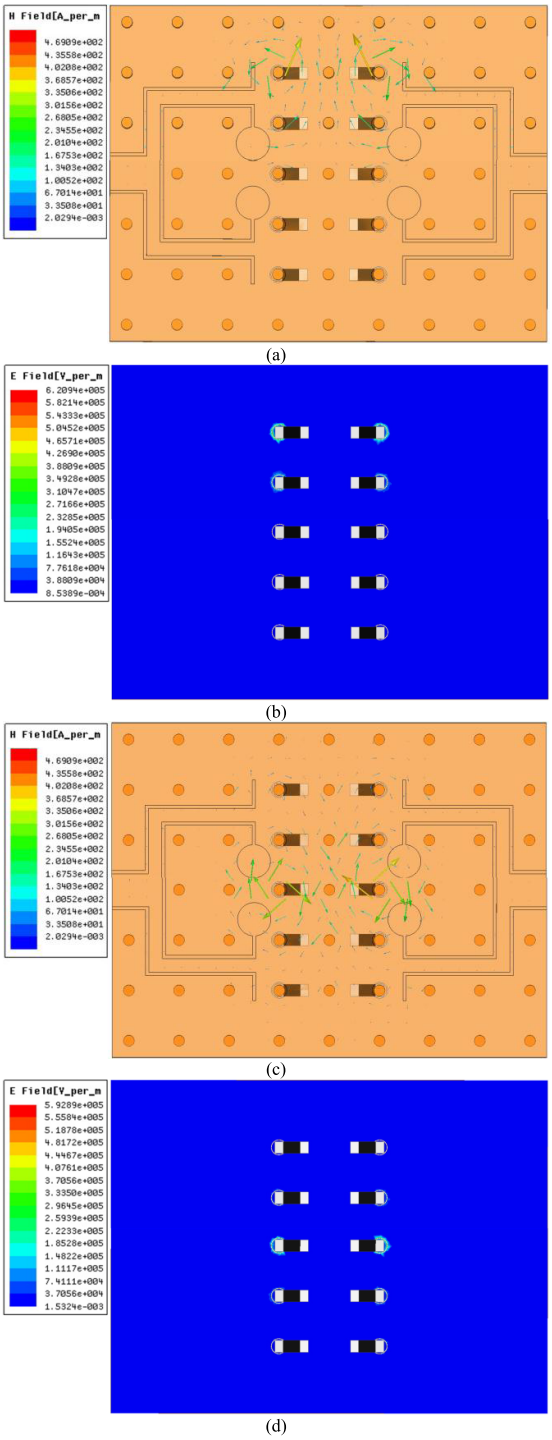

FIGURE 8. Simulated electric and magnetic fields in the quint-band filter: (a) and (b) Magnetic field vectors and electric fields at center frequency of third passband; (c) and (d) Magnetic field vectors and electric fields at center frequency of first passband.

The simulated magnetic and electric fields of a quint-band filter are shown in Fig. 8. With lumped capacitor's value of 4.8 pF, Res1 and Res2 are contributing the third passband with center frequency of 2.35 GHz. As shown in Fig. 8(a) and (b) simulated at 2.35GHz, the magnetic field vectors of the filter are mainly observed in the middle of resonant posts of Res1 and Res2, while electric fields mainly concentrate around air slots with surface mounted lumped capacitor. Examining another case, Res5 and Res6 with surface mounted capacitors of 11.6 pF give rise to the first passband with center frequency of 1.53 GHz. At 1.53 GHz, the filter's magnetic field vectors and electric fields are simulated shown in Fig. 8(c) and (d), illustrating the same observation of magnetic and electric field distribution as noted in 8(a) and (b). This confirms a low coupling coefficient among each passband filters in our design.

IV. EXPERIMENTAL RESULTS

Fig. 9 shows photographs of the fabricated filter with attached SMA connectors. Rogers RO4350 substrate with a dielectric constant of 3.66, a thickness of 1.524 mm and a loss tangent of 0.004 is used for experimental work. In implementing the filter, a standard two layer PCB process is used to construct the metal via posts, top and bottom metal plates.

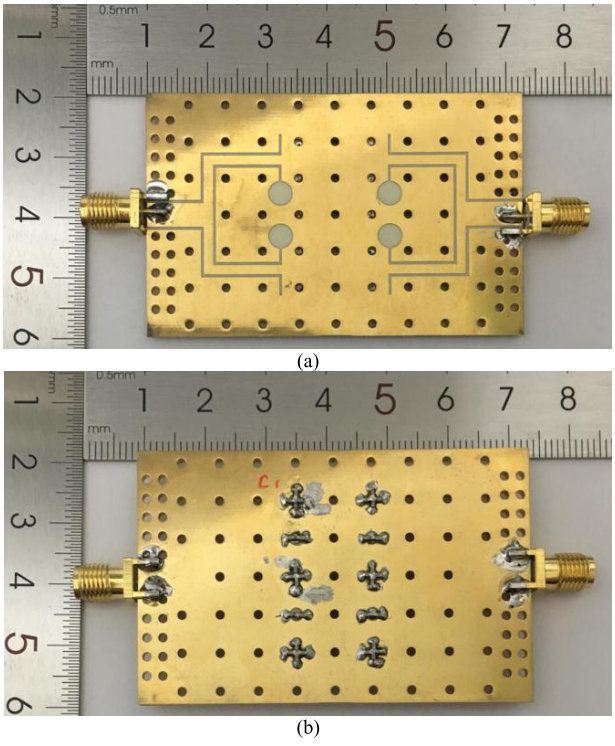

FIGURE 9. Photographs of fabricated CEBG quint-band filter: (a) Top view of filter; (b) Bottom view of filter.

ATC600L 0402 (0.5 mm × 1.0 mm) series lumped capacitors are chosen due to their small size and relatively high Q factor. Bottom view of the filter surface mounted by capacitors is shown in Fig. 9(b). Note that Q factor of a capacitor decreases as frequency increases and a capacitor with a smaller capacitance value yields a higher Q factor for a given frequency [18]. Please also note that filter's performance will be degraded by a low Q lumped capacitor. As presented in [9], insertion loss and Q_u of CEBG filter depend on Q factor of

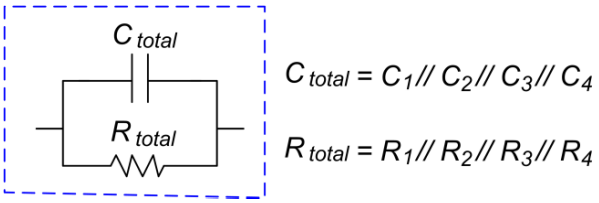

FIGURE 10. Equivalent circuit of four paralleled lumped capacitors.

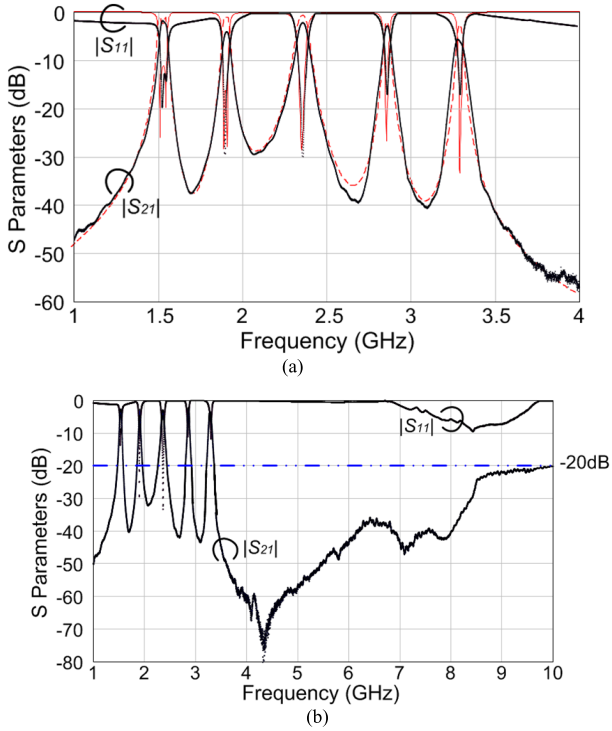

FIGURE 11. (a) Frequency responses of the designed (dash line) and fabricated (solid line) filters in the narrow band; (b) The frequency response of the fabricated filter in the wide band.

the surface mount lumped capacitor. As the Q of capacitor reduces, insertion loss and Q_u of the filter worsens while maintaining the same bandwidth. To obtain a big capacitance and high Q, small value lumped capacitors are connected in parallel shown in Fig. 9(b). Equivalent circuit of a parallel capacitor network is shown in Fig. 10.

Suppose capacitance value of every lumped capacitor is the same:

$$C_{total} = C_1 + C_2 + C_3 + C_4 = 4C_1 \tag{7}$$

$$R_{total} = \frac{R_1R_2R_3R_4}{R_2R_3R_4 + R_1R_3R_4 + R_1R_2R_4 + R_1R_2R_3} = \frac{R_1}{4} \tag{8}$$

Q of the capacitor network is :

$$Q(total) = \frac{\frac{1}{\omega_0 C_{total}}}{R_{total}} = \frac{1}{\omega_0 C_{total} R_{total}} = \frac{1}{\omega_0 C_1 R_1} = Q(C_1) \tag{9}$$

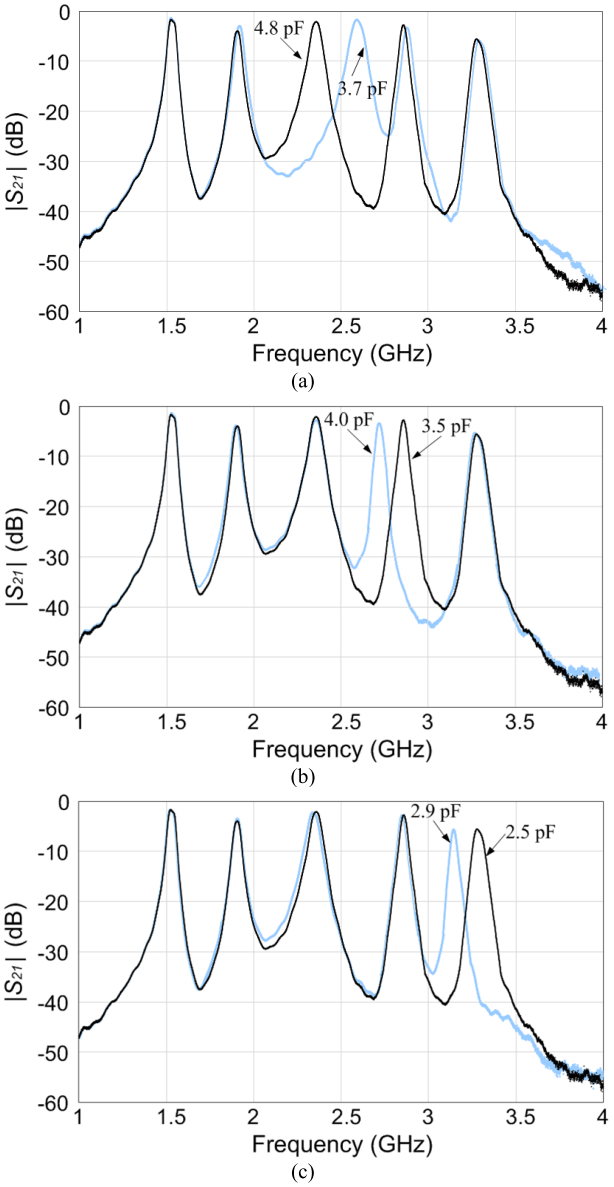

FIGURE 12. Measured working frequency change of individual passband with little influence on other passbands: (a) Third passband; (b) Fourth pandband; (c) Fifth passband.

From (9), the capacitor network with bigger capacitance value has same Q with a small value capacitor suggesting that the filter with surface mounted capacitor network work at low frequency with high Q. Since working frequency of the filter depends on the external capacitors and since it does not rely on size and height of via post, this design allows for an increased degree of design freedom. The fabricated filter was measured using an Agilent N5230C network analyzer. A short-open-load-through calibration was adopted for filter measurement.

Simulated and measured results of the quint-band filter are shown in Fig. 11. The five passbands centered at 1.53, 1.9, 2.35, 2.86, and 3.3 GHz have fractional bandwidth

of 1.91 %, 1.13 %, 1.62 %, 1.05 %, and 0.97 %. The measured minimum insertion losses of five passbands are 2.2, 3.6, 2.5, 2.6, and 5.4 dB respectively. Return losses of the five passbands are better than 13.0 dB. The measured loss is dominated by Q of lumped capacitors, which lead to an effective Q_u of 163 for the filter. From the measurement results, band to band isolation of the filter is better than 29.0 dB. The spurious signal suppression in the upper frequency range from 3.36 to 10.0 GHz is higher than 20.0 dB shown in Fig. 11(b). The effect of center frequency tuning of an individual band on other bands in our filter design is depicted in Fig. 12. Center frequency of one passband can be customizable adjusted without compromising performances of other four passbands. The performance attributes of our filter are compared with other multi-band filters is shown in Table 3. As can be seen, the proposed filter achieves state-of-the art performance with a compact footprint on the design, a wide spurious free range and five configurable passbands.

TABLE 3. Comparison with previous multi-band BPFs.

	RT	CFB	Pass band	Stop BW (-20 dB)	Center Freq. (GHz)	FBW (%)	Size (λ_g^2)
[1]	SIR	/	4	6.0-6.3	1.57/2.45/3.5/5.2	2.5/10/2.8/4	3.52
[2]	SIR	/	4	/	1.5/2.5/3.6/4.6	5.5/12/11/4.3	0.09
[3]	SIR	/	4	/	1.55/2.79/3.29/4.47	3.15/3.34/3.1/2.33	0.02
[4]	SIR	/	4	7.5-13.5	2.4/3.5/5.2/6.8	1.6/2.7/1/1.4	0.05
[5]	SIR	/	4	5.8-6.3	1.5/2.5/3.5/5.5	1.3/1.9/0.5/0.9	0.036
[8]	SIR	/	5	/	0.6/0.9/1.2/1.5/1.8	5.8/5.2/5.8/8/8	0.23
This work	**EBG**	**Yes**	**5**	**3.36-10.0**	**1.53/1.9/2.35/2.86/3.3**	**1.91/1.13/1.62/1.05/0.97**	**0.21**

RT: resonator type; CFB: configurable; BW: bandwidth; FBW: fractional bandwidth.

V. CONCLUSION

In this paper, a compact quint-band BPF has been presented based on EBG material with detailed design procedure and analysis. To the best of authors' knowledge, this is the first quint-band filter ever reported using EBG material. The proposed circuits successfully integrate five pairs of high Q EBG resonators into one quint-band BPF with good band to band isolation and without additional matching junction. Since each pair of resonators determines a respective passband characteristic, the proposed BPFs show high degree of design freedom. The frequency locations of all the passbands can be adjusted independently by controlling external lumped capacitor. Measured results reveal that the filter achieves a compact size, good quint-band performance, low insertion loss, good selectivity at passbands edges and wide stopband. This study provides a simple and effective method to design a quint-band bandpass filter without complex fabrication process. The superior features indicate that the proposed filter has a potential to be utilized in multi-service wireless communication systems.

ACKNOWLEDGMENT

This work is supported by the Natural Science Foundation of Jiangsu Province (BK20160190), the Fundamental Research Funds for the Central Universities (JUSRP11740), the Natural Science Foundation of China (61701195) and the Chinese Postdoctoral Science Foundation (2017M621710).

REFERENCES

[1] C.-M. Cheng and C.-F. Yang, "Develop quad-band (1.57/2.45/3.5/5.2 GHz) bandpass filters on the ceramic substrate," *IEEE Microw. Wireless Compon. Lett.*, vol. 20, no. 5, pp. 268–270, May 2010.
[2] J.-Y. Wu and W.-H. Tu, "Design of quad-band bandpass filter with multiple transmission zeros," *Electron. Lett.*, vol. 47, no. 8, pp. 502–503, Apr. 2011.
[3] S.-C. Lin, "Microstrip dual/quad-band filters with coupled lines and quasi-lumped impedance inverters based on parallel-path transmission," *IEEE Trans. Microw. Theory Techn.*, vol. 59, no. 8, pp. 1937–1946, Aug. 2011.
[4] H.-W. Wu and R.-Y. Yang, "A new quad-band bandpass filter using asymmetric stepped impedance resonators," *IEEE Microw. Wireless Compon. Lett.*, vol. 21, no. 4, pp. 203–205, Apr. 2011.
[5] K. W. Hsu and W. H. Tu, "Sharp-rejection quad-band bandpass filter using meandering structure," *Electron. Lett.*, vol. 48, no. 15, pp. 935–937, Jul. 2012.
[6] K.-W. Hsu, W.-C. Hung, and W.-H. Tu, "Compact quint-band microstrip bandpass filter using double-layered substrate," in *IEEE MTT-S Int. Microw. Symp. Dig.*, Boston, MA, USA, Jun. 2013, pp. 1041–1044.
[7] J. Ai, Y. Zhang, K. Da Xu, D. Li, and Y. Fan, "Miniaturized quint-band bandpass filter based on multi-mode resonator and λ/4 resonators with mixed electric and magnetic coupling," *IEEE Microw. Wireless Compon. Lett.*, vol. 26, no. 5, pp. 343–345, May 2016.
[8] C. F. Chen, "Design of a compact microstrip quint-band filter based on the tri-mode stub-loaded stepped-impedance resonators," *IEEE Microw. Wireless Compon. Lett.*, vol. 22, no. 7, pp. 357–359, Jul. 2012.
[9] Y. Guo, S. Kim, X. Liu, H. Gao, and G.-P. Li, "A compact configurable EBG filter on PCB," *IEEE Trans. Compon., Packag., Manuf. Technol.*, vol. 5, no. 5, pp. 668–674, May 2015.
[10] K. C. Gupta, R. Garg, I. Bahl, and P. Bhartia, *Microstrip Lines and Slotlines*, 2nd ed. Boston, MA, USA: Artech House, 1996, pp. 379–414.
[11] W. J. Chappell, M. P. Little, and L. P. B. Katehi, "High Q two dimensional defect resonators-measured and simulated," in *IEEE MTT-S Int. Microw. Symp. Dig.*, Boston, MA, USA, Jun. 2000, pp. 1437–1440.
[12] J. D. Joannopoulos, S. G. Johnson, J. N. Winn, and R. D. Meade, *Photonic Crystals: Molding the Flow of Light*, 2nd ed. Princeton, NJ, USA: Princeton Univ. Press, 2008, pp. 20–21.
[13] M. J. Hill, R. W. Ziolkowski, and J. Papapolymerou, "A high-Q reconfigurable planar EBG cavity resonator," *IEEE Microw. Wireless Compon. Lett.*, vol. 11, no. 6, pp. 255–257, Jun. 2001.
[14] K. J. Russell, "Microwave power combining techniques," *IEEE Trans. Microw. Theory Techn.*, vol. MTT-27, no. 5, pp. 472–478, May 1979.
[15] C.-H. Ho, L. Fan, and K. Chang, "Experimental investigations of CPW-slotline transitions for uniplanar microwave integrated circuits," in *IEEE MTT-S Int. Microw. Symp. Dig.*, Atlanta, GA, USA, Jun. 1993, pp. 877–880.
[16] J. Machac, J. Zehentner, and W. Menzel, "Short and open circuited slot line," in *Proc. SBMO/IEEE MTT-S Int. Microw. Optoelectron. Conf.*, Rio de Janeiro, Brazil, Jul. 1995, pp. 856–861.
[17] J.-S. Hong and M. J. Lancaster, *Microstrip Filters for RF/Microwave Applications*. New York, NY, USA: Wiley, 2001, pp. 235–271.
[18] American Technical Ceramics Corp. Multilayer Capacitors' Characteristics, USA. Accessed: Sep. 2, 2018. [Online]. Available: http://www.atceramics.com/multilayer_capacitors.html

YU GUO (M'18) was born in Xi'an, Shaanxi, China, in 1985. He received the B.S. degree in electrical engineering from Xidian University, Xi'an, China, in 2008, and the M.S. degree in electrical engineering from Southeast University, Nanjing, China, in 2011. From 2012 to 2015, he was an Exchange Ph.D. Student of electrical engineering and computer science at the University of California at Irvine, Irvine. During his stay, he was involved in the analysis and design of electromagnetic bandgap materials for tunable and configurable filters.

He holds one U.S. patent and six China patents with an additional three patents pending. He published over 20 research papers involving RF filter design and application. His current research interests include RF filter design and wireless system design and analysis.

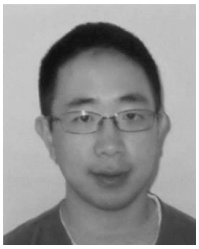

SUNGJUN KIM received the M.S. degree in electrical and electronics engineering from the State University of New York at Buffalo in 2006 and the Ph.D. degree in electrical engineering and computer science from the University of California at Irvine.

His current research interests include RF MEMS switch design, fabrication, and testing.

HUAI GAO (M'02–SM'09) received the B.S., M.S., and Ph.D. degrees in electrical engineering from Nanjing University, Nanjing, China, in 1983, 1993, and 2001, respectively. He is currently a Scientist with Nanjing University and Suzhou Innotion Technology Co., Ltd. He holds four U.S. patents. His research interest is on RF integrated circuit and MMIC design.

GUANN-PYNG LI (M'83) has served as a Research Staff Member and the Manager of the Technology Group, T. J. Watson Research Center, IBM, where he was involved in the area of VLSI technology and led a research and development team to transfer the technology into the marketplace. He is currently a Professor with the University of California at Irvine (UCI), Irvine, with appointments in three departments: Electrical Engineering and Computer Science, Chemical Engineering and Materials Science, and Biomedical Engineering. He also serves as the Division Director of the California Institute for Telecommunications and Information Technology (Calit2), UCI, where he is also the Director of the Integrated Nanosystems Research Facility, Henry Samueli School of Engineering. He has published over 380 research papers involving microelectronics, optoelectronic technologies, microwave circuit design, microelectro-mechanical systems for communication and biomedical instrumentation applications, and bio-nano-IT technology. He received the Outstanding Research Contribution Award from IBM (1987), two Outstanding Engineering Professor Awards from UCI (1997 and 2001), the UCI Innovators Award (2005), the Best Paper Award from the ITC International Telemetering Conference (2005), the Outstanding Asian American and Pacific Islander Community Leaders and Role Models Award by the Asian Business Association of Orange County (2009), and the Outstanding Alumni Award by the National Cheng Kung University Alumni Association of North America (2017). In the late 1980s, he chaired a committee charged with defining IBM's semiconductor technology roadmap beyond the year 2000. A member of numerous technical committees at professional conferences, he was the Chair of the Taiwan VLSI Technology, Circuit, and System Conference in 2006. He has also served as the Chair of the Executive Committee for Electronics Manufacturing Research and New Materials, University of California (2004–2006).

He also directs TechPortal, a technology business incubator housed at the UCI division of Calit2, which supports and nurtures young companies and university researchers commercializing their technologies. He holds 33 U.S. patents with an additional 15 patents pending and has started several companies based on his inventions. His current research interests focus on the developing Internet of Things technologies for efficient energy utilization, smart manufacturing, and e-health. He was one of four engineering professors honored at the UCI Innovations Ceremony in recognition of their significant contributions to the university as inventors and creators in 2005.